Journal of Medicinal Chemistry

Article

Synthesis of Leukotriene B4 Antagonists Labeled with In-111 or Tc-99m to Image Infectious and Inflammatory Foci

Matthias Broekema, Jullitte J. E. M. van Eerd, Wim J. G. Oyen, Frans H. M. Corstens, Rob M. J. Liskamp, Otto C. Boerman, and Thomas D. Harris

J. Med. Chem., **2005**, 48 (20), 6442-6453• DOI: 10.1021/jm050383h • Publication Date (Web): 01 September 2005

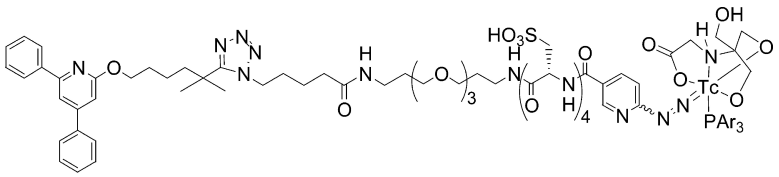

PAr_3 = trisodium triphenylphosphine-3,3',3"-trisulfonate (TPPTS)

More About This Article

Additional resources and features associated with this article are available within the HTML version:

- Supporting Information
- Links to the 1 articles that cite this article, as of the time of this article download
- Access to high resolution figures
- Links to articles and content related to this article
- Copyright permission to reproduce figures and/or text from this article

View the Full Text HTML

Journal of Medicinal Chemistry is published by the American Chemical Society. 1155 Sixteenth Street N.W., Washington, DC 20036

Synthesis of Leukotriene B4 Antagonists Labeled with In-111 or Tc-99m to Image Infectious and Inflammatory Foci

Matthias Broekema,[§,†] Julliëtte J. E. M. van Eerd,[‡] Wim J. G. Oyen,[‡] Frans H. M. Corstens,[‡] Rob M. J. Liskamp,[†] Otto C. Boerman,[‡] and Thomas D. Harris[§,*]

Bristol-Myers Squibb Medical Imaging, North Billerica, Massachusetts 01862, Department of Medicinal Chemistry, Utrecht Institute for Pharmaceutical Sciences, Utrecht University, Utrecht, The Netherlands, and Department of Nuclear Medicine, University Medical Center Nijmegen, The Netherlands

Received April 22, 2005

In previous studies we demonstrated that lipophilic ^{99m}Tc-labeled LTB_4 antagonist **1** (RP517) accumulated in infectious foci in rabbits, but hepatobiliary clearance hampered imaging of abdominal lesions. We now report the use of cysteic acid as a pharmacokinetic modifier to improve the water solubility and renal clearance of three hydrophilic analogues of **1**. Divalent LTB4 antagonist **17** (DPC11870-11) is a DTPA conjugate for radiolabeling with In-111. Monovalent LTB_4 antagonists **15** (BMS57868-88) and divalent LTB_4 antagonist **18** (BMS57868-81) are conjugated to bifunctional chelator HYNIC for radiolabeling with ^{99m}Tc. The three compounds labeled efficiently with ^{111}In or ^{99m}Tc with high radiochemical purity and specific activities. Scintigraphic images obtained in New Zealand White rabbits having acute intramuscular *E. coli* infection demonstrated that all agents were able to clearly visualize the abscess, and clearance was exclusively renal. The biodistribution of the ^{99m}Tc-labeled LTB_4 antagonists was affected by the coligands used with the HYNIC chelator and by the monovalent or divalent nature of the receptor binding moiety. The best scintigraphic images were obtained with monovalent HYNIC conjugate **15** using tricine and isonicotinic acid as coligands with HYNIC for coordination with ^{99m}Tc.

Introduction

The leukotriene B_4 (LTB_4) receptors are G-protein-coupled receptors (GPCR) that are involved in recruitment and activation of leukocytes during an inflammatory response.[1] At present, two LTB_4 receptor types are identified, BLT_1 and BLT_2, which have different affinities for LTB_4.[2,3] The high affinity receptor BLT_1 is mainly expressed on neutrophils, while BLT_2 is expressed more ubiquitously. LTB_4 plays an essential regulatory role during the inflammatory response. However, its overproduction is reported to play a role in pathological conditions such as asthma, inflammatory bowel disease and arthritis.[4,5] Consequently, a large number of LTB_4 antagonists have been developed for clinical application as antiinflammatory therapeutics.[6] The rapid detection of infectious and inflammatory foci in patients is essential for timely and adequate therapeutic intervention. One of the current methods for detection of infection and inflammation is scintigraphic imaging. The generally used radiopharmaceuticals for this purpose, ^{99m}Tc-labeled leukocytes and ^{67}Ga-citrate, have several disadvantages. The blood handling required for the preparation of radiolabeled leukocytes is accompanied by the risk of infection from blood-borne pathogens, and is a time-consuming preparation.[7,8] The nuclear and biodistribution properties of ^{67}Ga-citrate are far from ideal, resulting in poor image quality and increased radiation burden to the patient.

We previously reported on the synthesis and imaging properties of ^{99m}Tc-labeled LTB_4 antagonist **1** (Figure 1).[9] LTB_4 antagonist **2** (RPR69698)[10] was modified with a short PEG spacer to give compound **3**, and the Boc group of **3** was replaced with the bifunctional chelator hydrazinonicotinic acid (HYNIC) to give drug precursor **4**. The hydrazine was protected as the hydrazone of sodium 2-formylbenzenesulfonate to avoid reaction with trace quantities of formaldehyde and other carbonyl compounds commonly found in the research and manufacturing environment.[11] The radiolabeling of **4** utilized ^{99m}Tc$[TcO_4]^-$ in the presence of coligands tricine and trisodium triphenylphosphine-3,3′,3″-trisulfonate (TPPTS).[12] This radiolabeling procedure gave a rapid and clean formation of ternary ligand complex **1**. This tracer showed rapid accumulation in the infected thigh muscle in the rabbit *E. coli* model.[13] However, **1** clears almost exclusively via the hepatobiliary route, and physiologic uptake in the intestines limits clinical applicability of this agent. On the basis of these observations, more hydrophilic compounds were designed, using cysteic acid (Csa) as a pharmacokinetic modifier (PKM). Initially, compound **3** was modified with four cysteic acids, converted to a divalent ligand using glutamic acid, and conjugated to DTPA giving **17** (Scheme 3). The ^{111}In complex of **17** (**23** in Figure 2) was found to rapidly visualize infectious foci in the rabbit *E. coli* infected thigh muscle model.[14] Uptake in the infectious foci was reduced 88% by preinjection with an excess of nonradioactive [In(**17**)]. This indicated that the interaction of the radiolabeled agent in the infected

* To whom correspondence should be addressed: Thomas Harris, Bristol-Myers Squibb Medical Imaging, 331 Treble Cove Rd., North Billerica, MA 01862. E-mail: thomas.d.harris@bms.com. Phone: 978-671-8266. Fax: 978-436-7500.
§ Bristol-Myers Squibb Medical Imaging.
† Utrecht University.
‡ University Medical Center Nijmegen.

10.1021/jm050383h CCC: $30.25
Published on Web 09/01/2005

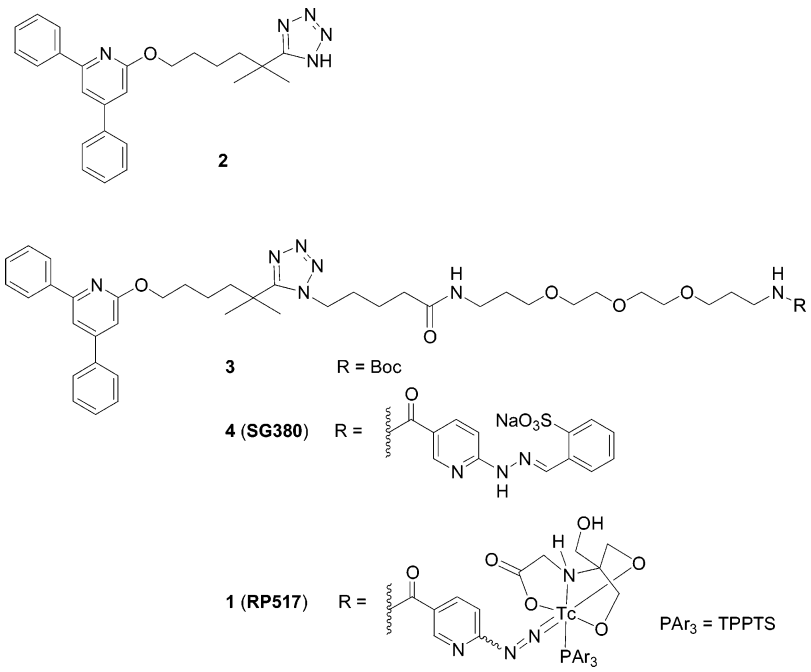

Figure 1. Structures of lead LTB$_4$ antagonist **2**, PEG-modified LTB$_4$ antagonists **2**, protected HYNIC derivative **4**, and ^{99m}Tc ternary ligand complex **1**.

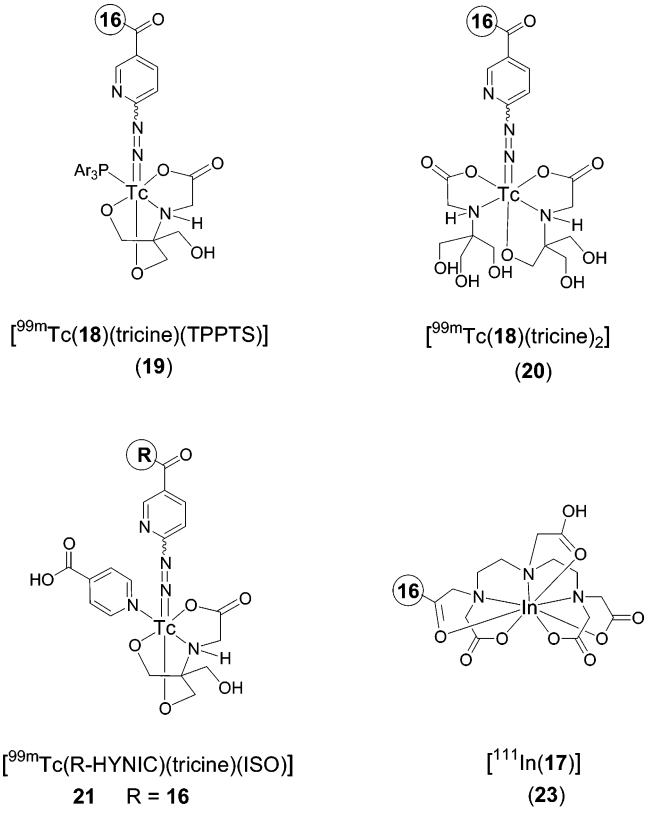

Figure 2. Comparison of the structures of [^{99m}Tc(HYNIC)-(L_1)(L_2)] complexes and [^{111}In(**17**)] (**23**).

tissue was receptor-specific and that the interaction was saturable. The agent clears rapidly from nontarget tissues, and excretion is almost exclusively renal.

Although the biodistribution and imaging properties of **23** are very promising, a ^{99m}Tc-labeled tracer is generally preferred for scintigraphic imaging over an ^{111}In-labeled tracer because of the more favorable nuclear properties of ^{99m}Tc (140 keV gamma emissions, 6 h half-life) and the general availability of portable ^{99m}Tc generators. Herein we describe the synthesis and initial biological evaluation of two analogues of **17**. One compound (**18**) is structurally almost identical to **17**, with HYNIC replacing DTPA, while the other compound (**15**) is a monovalent version of **18**. Both of these LTB$_4$ antagonists were radiolabeled with ^{99m}Tc, and the in vivo imaging characteristics were compared with those of **23**. Furthermore, using divalent HYNIC conjugate **18**, we have compared the biodistribution properties of three coligand systems and shown that the coligand system can have a profound effect on the biodistribution properties of these ^{99m}Tc complexes. We also describe the complete synthesis of **17** and provide an improved synthesis of PEGylated LTB$_4$ antagonist **3**.

Results

Synthesis. PEG-modified LTB$_4$ antagonist **3** was synthesized as outlined in Scheme 1. The tetrazole ring of **2** was alkylated with ethyl 5-bromovalerate in cyclohexane. Selectivity for alkylation at the N1 position was increased by blocking the N2 position with the tri-*n*-butyltin group.[15] Flash chromatography gave a 36% yield of the desired N1-alkylation product **5a**, along with 22% of the unwanted N2 isomer **5b**. The ester group of **5a** was hydrolyzed with LiOH in aqueous THF to give a quantitative yield of compound **6**. Conjugation of **6** with *N*-(*tert*-butoxycarbonyl)-4,7,10-trioxa-1,13-tridecanediamine using HBTU coupling reagent afforded a 99% yield of **3**.

The tetracysteic acid derivative of **3** was synthesized by the sequential coupling of four Boc-cysteic acid-mono sodium salt residues (Boc-Csa(Na)-OH) as shown in Scheme 1. The Boc-protecting group of **3** was removed using a mixture of trifluoroacetic acid (TFA), dichloromethane (DCM), water, and triisopropylsilane (TIS). The amine TFA salt (**7**) resulting after concentration of the reaction solution was used without purification. Boc-Csa(Na)-OH was preactivated using HBTU, and DIEA

Scheme 1. Synthesis of Tetra-Cysteic Acid-Modified LTB_4 Antagonist **13**[a]

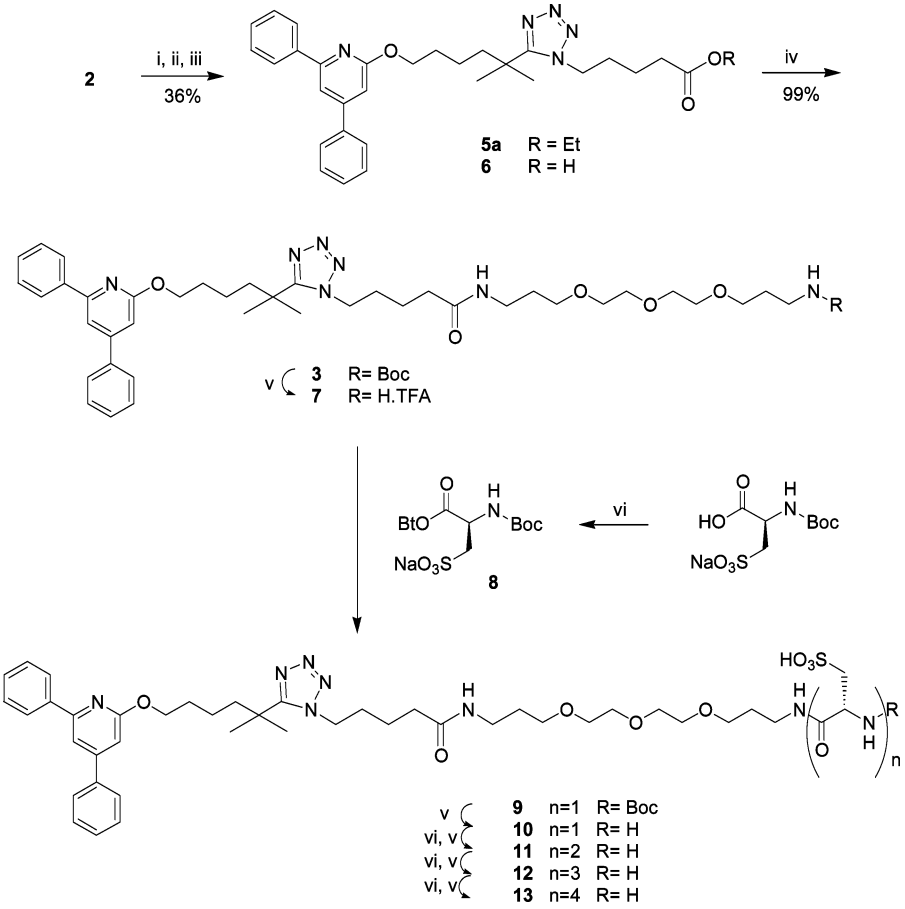

[a] Reagents: (i) bis(tri-*n*-butyltin)oxide, EtOH; (ii) ethyl 5-bromovalerate, cyclohexane, 36%; (iii) aq LiOH, THF, 100%; (iv) *N*-(*tert*-butoxycarbonyl)-4,7,10-trioxa-1,13-tridecanediamine, HBTU, DIEA, 99%; (v) TFA, DCM, TIS, water; (vi) Boc-Csa(Na)-OH, HBTU, DIEA, DMF.

Scheme 2. Synthesis of Monovalent HYNIC Conjugate **15**[a]

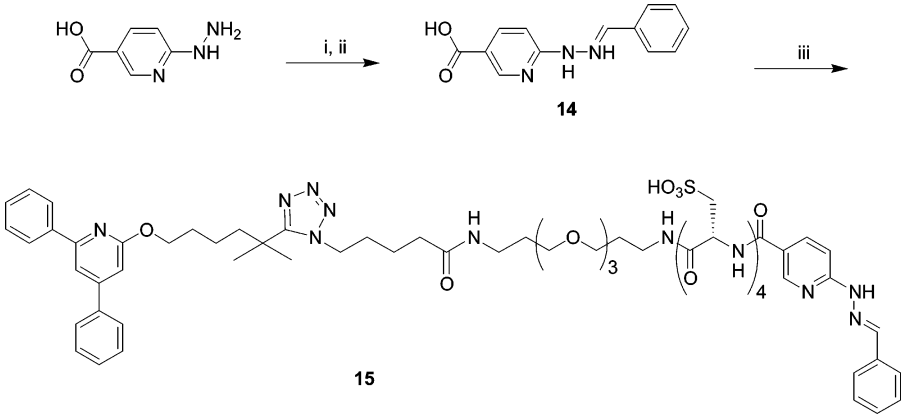

[a] Reagents: (i) benzaldehyde, DMF; (ii) DCM wash, 66%; (iii) **13**, PyBOP, DIEA, DMF, 30%.

in DMF solution, and the resulting *N*-hydroxybenzotriazole ester (**8**) was added to a solution of **7** in DMF. The resulting Boc-protected cysteic acid derivative (**9**) was purified my means of extraction into $CHCl_3$ and washing with H_2O and saturated $NaHCO_3$. The saturated $NaHCO_3$ wash removed the 1-hydroxybenzotriazole (HOBt) from the organic layer, and the crude product was used without further purification. The Boc group of compound **9** was removed as described above giving **10**. The products of the second, third, and fourth deprotection/cysteic acid coupling cycles (**11**, **12**, and **13**, respectively) were too hydrophilic for purification by partitioning between aqueous and organic phases, and therefore were purified by preparative reverse phase HPLC on a C18 column. Products were recovered from the aqueous eluants by lyophilization and were obtained as flocculent colorless solids.

6-Hydrazinonicotinic acid was converted to 6-(2-benzaldehydehydrazono)nicotinic acid (**14**) using an excess of benzaldehyde as shown in Scheme 2.[11,16] Unreacted benzaldehyde was removed by trituration with DCM to give pure **14** in 66% yield. The conjugation reaction between **13** and **14** was mediated with benzotriazol-1-yl-oxytripyrrolidinophosphonium hexafluoro-

Scheme 3. Synthesis of Divalent DTPA Conjugate **17** and Divalent HYNIC Conjugate **18**[a]

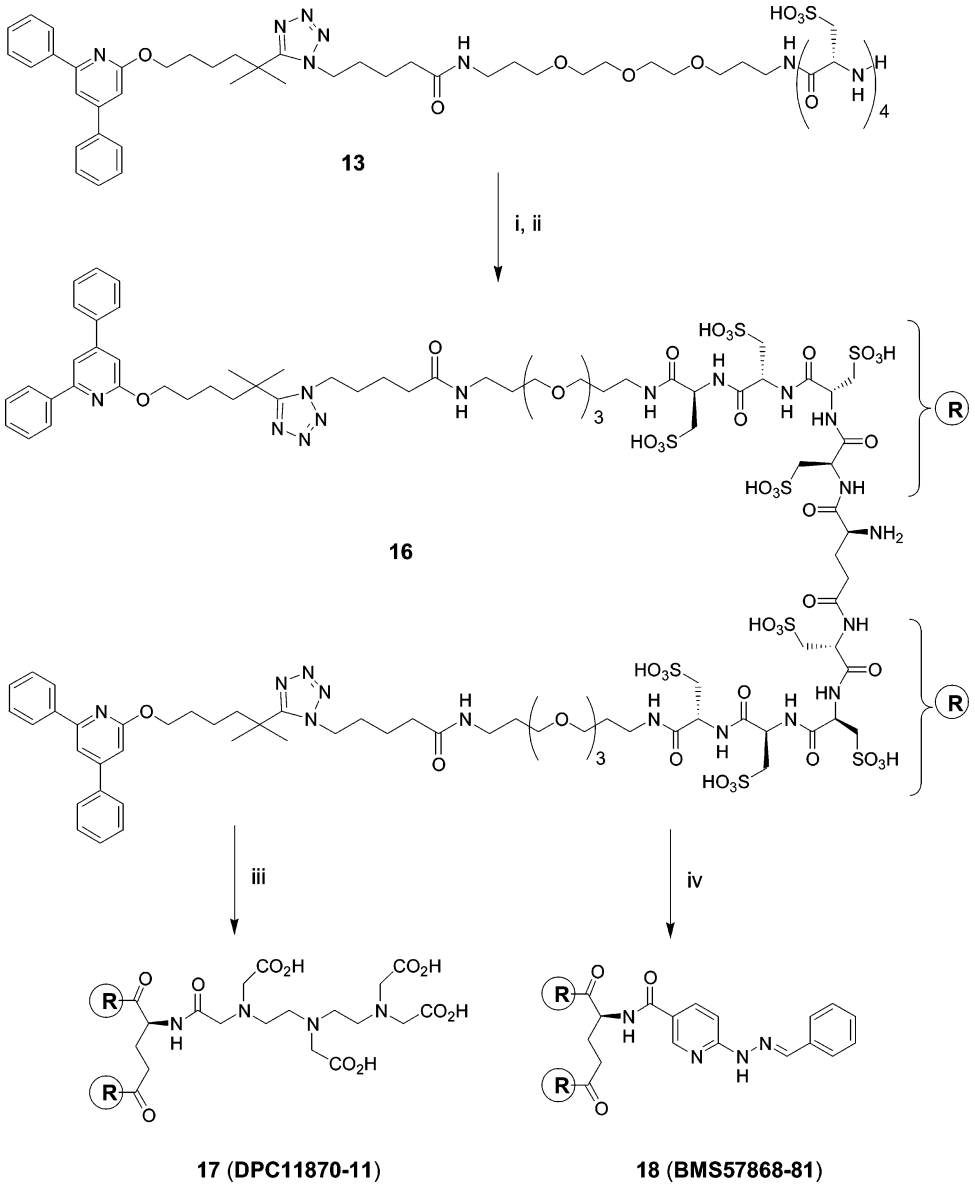

[a] Reagents: (i) Boc-Glu(OTfp)-OTfp, HOAt, DIEA, DMF; (ii) TFA, DCM, 62%; (iii) DTPA dianhydride, DIEA, DMF, 96%; (iv) 6-(2-benzaldehydehydrazono)nicotinic acid (**14**), PyBOP DIEA, DMF, 78%.

phosphate (PyBOP) and DIEA in DMF solution to give a 30% purified yield of **15**.

Preparation of the divalent LTB$_4$ antagonist was achieved by the conjugation of tetracysteic acid derivative **13** to both of the carboxylic groups of Boc-glutamic acid, using Boc-Glu(OTfp)-OTfp as the activated form (Scheme 3). The addition of HOAt significantly increased the reaction rate, and the reaction was complete in 6 h at ambient temperatures. The Boc group was removed using a cocktail of TFA/DCM/water/anisole, and the resulting amine was purified by HPLC to give a 62% yield of divalent LTB$_4$ antagonist **16** as a flocculent, colorless solid. Compound **16** was used for the preparation of divalent DTPA conjugate **17** and divalent HYNIC conjugate **18**. Reaction of **16** with DTPA dianhydride in DMF gave a 96% yield of **17** after HPLC purification. HYNIC conjugate **18** was isolated in 78% yield by a PyBOP-mediated coupling of **16** and **14** in DMF.

Receptor Binding Assay. The IC$_{50}$ values for all of the chelator conjugates described here were obtained in a competition assay with [^{111}In(**17**)]. As shown in Table 1, the receptor affinities of monovalent conjugates **4** and **15**, and divalent DTPA conjugate **17**, were nearly identical to that of parent LTB$_4$ antagonist **2**. Divalent HYNIC conjugate **18** showed a greater than 10-fold loss of receptor affinity.

Table 1. IC$_{50}$ Values (nM) of Chelator Conjugates

	competing agent	
compound	[^{3}H]LTB$_4$	[^{111}In(**17**)]
2	20[a]	
4	45 (n = 4)[b]	44 (n = 2)
16	8 (n = 2)[b]	
17	54 (n = 2)[b]	30 (n = 2)
15		16 (n = 2)
18		230 (n = 2)

[a] Reference 10. [b] NovaScreen, Hanover, MD.

Radiolabeling. HPLC analyses, performed after ^{99m}Tc-labeling of divalent HYNIC-conjugated compound **18**, indicated that with all three coligand systems the compound labeled at a specific activity of 37 MBq/μg

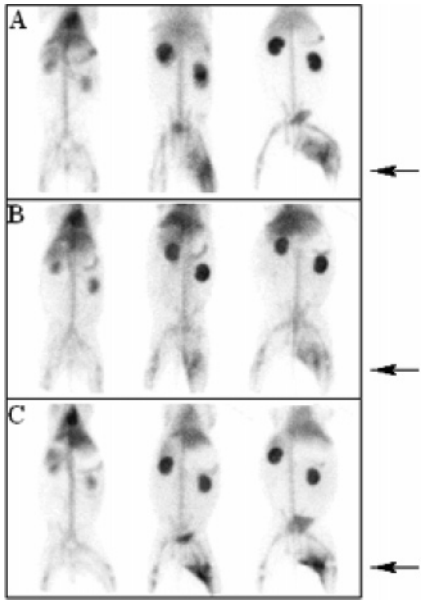

Figure 3. Anterior images of rabbits induced with an intramuscular infection. Images were acquired immediately, 4, and 8 h pi of 37 MBq divalent imaging agent [^{99m}Tc(**18**)], radiolabeled using tricine/TPPTS (**19**) (A), tricine$_2$ (**20**) (B), and tricine/ISO (**21**) (C) coligand systems.

(110 MBq/nmol) with a labeling efficiency >95%. Monovalent HYNIC-conjugated LTB$_4$ antagonist **15** labeled at a specific activity of 110 MBq/nmol with a labeling efficiency >95%. Divalent DTPA-conjugated LTB$_4$ antagonist **17** was labeled with ^{111}In at a specific activity of 12 MBq/nmol with a labeling efficiency >95%.

Animal Studies. Divalent HYNIC-modified LTB$_4$ antagonist **18** was radiolabeled with ^{99m}Tc using three different coligand systems, tricine/TPPTS, tricine$_2$, and tricine/ISO, to give complexes of the general formula [^{99m}Tc(**18**)L$_1$L$_2$]. The structures of these three ligand systems are shown in Figure 2. Pharmacokinetics of these three tracers were studied in three groups of rabbits with *E. coli* infection, with images acquired 5 min, 4 and 8 h postinjection (pi). As shown in Figure 3, immediately after injection the distribution of [^{99m}Tc(**18**)L$_1$L$_2$] was similar for all three coligand systems. Uptake of the tracer was observed in the heart, lungs, liver, and kidneys and in the bone marrow. At 4 h and especially at 8 h after injection of the compounds, the radioactivity had accumulated in the abscess resulting in clear delineation of the infectious lesions. The images acquired at 8 h pi clearly indicated that the coligand used during the labeling procedure affected the in vivo distribution of the LTB$_4$ antagonist. Visualization of the abscess was better when TPPTS or ISO was used as coligand in combination with tricine, than when tricine was used alone.

Ex vivo biodistribution determination of radioactivity concentration in the dissected tissues confirmed the observations in the imaging experiment (Figure 4). Radioactivity concentrations in the abscess were highest when [^{99m}Tc(**18**)] was labeled with the tricine/TPPTS and tricine/ISO coligand systems. Uptake in nontarget organs was also affected by the coligand system. The radioactivity concentration in the spleen and kidneys was significantly higher using tricine/TPPTS coligands, as compared to the uptake in these organs using tricine/ISO or tricine alone ($p < 0.01$). Altogether, the abscess

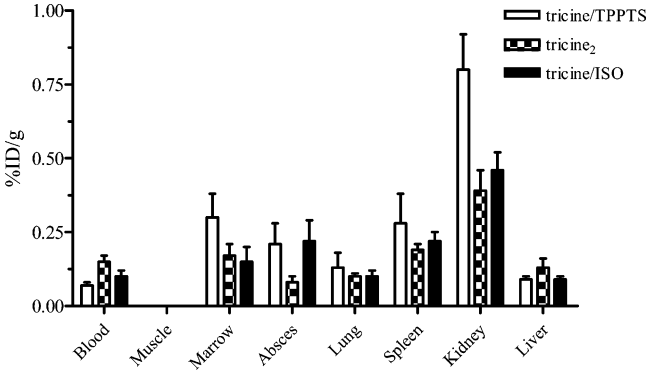

Figure 4. Biodistribution data obtained 8 h pi using divalent imaging agent [^{99m}Tc(**18**)] radiolabeled using tricine/TPPTS (**19**), tricine$_2$ (**20**), and tricine/ISO (**21**) coligand systems. Each bar represents the mean values ± SD.

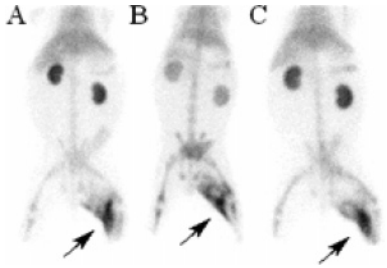

Figure 5. Comparison of divalent imaging agent [^{99m}Tc(**18**)-(tricine)(ISO)] (**21**) (A), monovalent imaging agent [^{99m}Tc(**15**)(tricine)(ISO)] (**22**) (B), and divalent imaging agent [^{111}In(**17**)] (**23**) (C). All are anterior images of rabbits induced with an intramuscular infection. Images were acquired 8 h pi of 37 MBq for (A) and (B) and 11 MBq for (C).

visualization was best after injection of [^{99m}Tc(**18**)-(tricine)(ISO)] (**21**), because this preparation combined high uptake in the abscess with low radioactivity concentration in nontarget tissues, particularly in the kidneys.

In the next imaging experiment, rabbits with intramuscular infection were injected with either the divalent or monovalent ^{99m}Tc-labeled LTB$_4$ antagonist [^{99m}Tc-(**18**)(tricine)(ISO)] (**21**) or [^{99m}Tc(**15**)(tricine)(ISO)] (**22**), respectively) or with the ^{111}In-labeled divalent LTB$_4$ antagonist [^{111}In(**17**)] (**23**). The images acquired at 8 h pi showed that all three tracers visualized the intramuscular abscess (Figure 5). When the three agents were compared, it appeared that the distribution of both divalent analogues was very similar. All three analogues clearly delineated the intramuscular abscess. Nontarget uptake of radioactivity for the three agents was similar in bone marrow, liver, and spleen. However, the kidney uptake of monovalent agent [^{99m}Tc(**15**)(tricine)(ISO)] (**22**) appeared to be significantly lower.

Discussion

Leukotriene B4 (LTB$_4$) is a potent pro-inflammatory lipid mediator derived from arachidonic acid via the 5-lipoxygenase pathway. It is produced by neutrophils, monocytes, macrophages, keratinocytes, lymphocytes, and mast cells. The physiological responses to LTB$_4$ include potent neutrophil chemotactic activity, adhesion of PMNs to the vascular endothelium, stimulation of the release of lysosomal enzymes and superoxide radicals by PMNs, and an increase in vascular permeability. Increased levels of LTB$_4$ have been detected in patients

with asthma, acute respiratory distress syndrome, chronic obstructive pulmonary disease, contact dermatitis, cystic fibrosis, inflammatory bowel disease, gout, myocardial ischemia, psoriasis, rheumatoid arthritis, and cancer. Thus, it is widely believed that LTB_4 is an important mediator of acute and chronic inflammatory events. This has made the LTB_4 receptor the target of intense research by major pharmaceutical companies for therapeutic applications, and in recent years, a number of highly potent and selective LTB_4 antagonists have been reported. These compounds have been shown to be safe and efficacious in both animal models and in humans.[6,17,18] This wealth of information on LTB_4 antagonists made the LTB_4 receptor the most attractive of the various approaches available for the development of a neutrophil-binding radiolabeled infection/inflammation imaging agent.

In the present study the syntheses of three structurally related LTB_4 antagonists are described. These antagonists were designed for scintigraphic visualization of infectious and inflammatory foci. In the field of nuclear medicine, there is an ongoing search for the ideal radiopharmaceutical to visualize infectious and inflammatory foci. For this purpose many radiolabeled peptides, cytokines, and antagonists have been studied.[8] In our original work in this area we synthesized LTB_4 antagonist **4** (Figure 1), for the visualization of infectious and inflammatory lesions. This compound was based on **2**, a lipophilic BLT_1 receptor-binding ligand.[10] Compound **4** is a conjugate of bifunctional chelator hydrazinonicotinic acid (HYNIC) to allow efficient radiolabeling with ^{99m}Tc. The ternary ligand complex of **4**, utilizing TPPTS and tricine as coligands (**1** in Figure 1), accumulated rapidly in infected tissues containing infiltrated BLT_1-positive neutrophils.[12,13] However, due to the lipophilicity of the receptor binding moiety of **1**, the tracer cleared via the hepatobiliary route, and the rapid physiologic uptake of the tracer in the liver and the intestines interfered with visualization of inflammatory lesions in the abdomen.[13]

Various strategies have been used to enhance the hydrophilicity of radiopharmaceutical drugs, to increase their water solubility and/or renal clearance. These include the introduction of polar function groups (carboxyl, amine, etc.)[19] and PEG chains,[20] and the use of different radionuclide chelators.[21] Our experience with **4** indicated that we were unlikely to achieve a significant change in solubility or biodistribution properties by the introduction of simple PEG tethers. Here we present the synthesis and characterization of three hydrophilic tracers (**17**, **18**, and **15** in Schemes 2 and 3) based on the same receptor binding moiety used in the synthesis of **4**. The lipophilicity of **4** was reduced by the introduction of multiple cysteic acids as a PKM. Cysteic acid was chosen for this role because of the high polarity of the sulfonic acid group and because it is an unnatural amino acid and is therefore less likely to undergo metabolism. We have also examined the effect of two different radionuclide chelators (DTPA for coordination to ^{111}In, and HYNIC for coordination to ^{99m}Tc) because it is known from other studies that the chelator can influence the biodistribution of the tracer.[21] Finally, we have examined the effect of different coligands with HYNIC because previous reports have shown that the nature of the coligand can have a marked effect on biodistribution.[22,23]

In our original synthesis of **4** the tetrazole ring of **2** was alkylated with ethyl 5-bromovalerate in refluxing ACN in the presence of DIEA as base.[24] Alkylation of 5-substituted tetrazoles under these conditions always produces the N2 isomers in greater proportion than the N1 isomers. In our original synthesis the N1/N2 ratio was a very unfavorable 0.14. We subsequently learned that the product ratio can be shifted in favor of the N1 isomer by blocking the N2 position with the tri-*n*-butyltin group.[15] Preparation of the 2-(tri-*n*-butylstannyl)tetrazole was accomplished by treatment of **2** with bis(tri-*n*-butyltin)oxide in refluxing EtOH (Scheme 1). The EtOH solvent was replaced with cyclohexane, ethyl 5-bromovalerate was added, and the solution was heated to reflux. The reaction solution was then diluted with ether and washed with aqueous KF to remove tin byproducts. Final purification by flash chromatography gave a 36% yield of the N1 isomer (**5a**) and a more favorable N1/N2 ratio of 1.64. We discovered that formation of the N1 isomer is favored by the use of nonpolar solvents, and that even trace quantities of EtOH remaining from the formation of the 2-(tri-*n*-butylstannyl)tetrazole have a negative effect on the yield of the N1 isomer. Structure assignments were based upon the observation that the NMR chemical shift of the N1-alkyl substituents is 0.15−0.35 ppm upfield from that of the N2 isomer.[25] With this improvement over our original synthesis we were able to carry out the tetrazole alkylation on a relatively large scale, producing 16.58 g of purified **5a**. The remaining steps in the synthesis of compound **3** followed our original procedures, as described in the Experimental Section. The four cysteic acid PKMs were added stepwise to **3** in a series of deprotection/coupling cycles, as shown in Scheme 1. Boc-Csa(Na)-OH was preactivated using HBTU, and the resulting *N*-hydroxybenzotriazole ester (**8**) was added to a DMF solution of the amine. After the addition of one cysteic acid residue (i.e., **9**, R = Boc), the product was still sufficiently lipophilic that polar byproducts could be removed by water washes. But subsequent cysteic acid coupling cycles gave products that were too hydrophilic for an aqueous workup procedure. These compounds were deprotected, and the products (i.e., **11**, **12**, **13**) of these reactions were purified by reverse phase HPLC and isolated from the eluants by lyophilization. The overall yield for these four coupling cycles was 37%.

The biomolecules employed as the basis for development of radiopharmaceuticals are frequently very potent and elicit a biological response even at low doses. Radiolabeling in the clinical setting must therefore be carried out using very small quantities of the biomolecule, and a substantial effort has been made to find radionuclide chelators that can be easily radiolabeled in aqueous solution at very low concentrations of the biomolecule and with high specific activity. One of the best chelators for ^{99m}Tc is 6-hydrazinonicotinic acid (HYNIC), which is efficiently labeled in aqueous solutions having a ligand concentration as low as 10^{-5} M.[12] Protection of the hydrazine group of HYNIC during conjugation to the targeting molecule is essential in order to prevent unwanted conjugation reactions. Pro-

tection is also desirable during manufacturing of the lyophilized kit used for preparation of the radiopharmaceutical, because the hydrazine moiety reacts readily with aldehydes and ketones found in the manufacturing environment. Such materials are extracted from various rubber and plastic materials and are also used in common disinfectants. Formaldehyde is particularly ubiquitous. In our initial work in this area we discovered that hydrazones of aromatic aldehydes were particularly useful as hydrazine protecting groups on HYNIC.[11] These hydrazones are stable during synthesis and HPLC purification and protect the hydrazine moiety from reaction with common carbonyl impurities. The hydrazone is spontaneously cleaved during the radiolabeling process allowing formation of the diazenidotechnetium bond. We found that the hydrazone of sodium 2-formylbenzesulfonate was especially useful because the sulfonate group greatly improved water solubility of the HYNIC conjugate (see Figure 1). With multiple cysteic acid PKMs present on the LTB_4 antagonists described here, a further increase in water solubility was unnecessary, and we used the simpler hydrazone of benzaldehyde for protection of the hydrazine moiety (**14** in Scheme 2). Conjugation of **14** to tetracysteic acid derivative **13** was accomplished using PyBOP to give a 30% purified yield of **15**.

Many interactions in biological systems are polyvalent in nature (e.g., DNA helix, carbohydrate interactions, virus-cell wall interactions). However, it is only recently that polyvalency has begun to be explored in drug development.[26] In previous studies we have shown that divalency of a cyclic RGD peptide targeting the vitronectin receptor on tumors caused enhanced receptor affinity and enhanced retention in the target tissue in vivo.[27] We have explored the effect of divalency in these radiolabeled LTB_4 antagonists by preparing the pseudodimer of **13**. Tetracysteic acid derivative **13** was efficiently converted to a divalent ligand by reaction with Boc-Glu(OTfp)-OTfp and HOAt in DMF (Scheme 3). The HOAt greatly accelerated the reaction rate, reducing the reaction $t_{1/2}$ from 12 to 1 h. Removal of the Boc protecting group gave a 62% yield of **16** after HPLC purification. Conjugation of **16** to DTPA was accomplished by using a 10-fold excess of DTPA dianhydride and gave a 96% purified yield of **17**. Conjugation of **16** to **14** gave a 78% purified yield of divalent HYNIC conjugate **18**.

The IC_{50} values of the chelator conjugates reported in this study are shown in Table 1. Lipophilic HYNIC conjugate **4** has a receptor affinity of 45 nM, which is only slightly weaker than the 20 nM value of parent LTB4 antagonist **2**. Divalent water-soluble amine **16** shows a slight increase in receptor affinity to 8 nM, while the corresponding DTPA conjugate (**17**) shows a slight loss of affinity to 54 nM. These data confirm our original hypothesis that the LTB_4 receptor is very tolerant of substitutions on the tetrazole ring. Monovalent water-soluble HYNIC conjugate **15** has affinity of 16 nM, but surprisingly the divalent version (**18**) shows a large loss of receptor affinity with an IC_{50} value of 230 nM. Comparison with the affinities of the other divalent LTB_4 antagonist (**17**) suggests this is not due solely to the divalent nature of the molecule, and comparison with the other two HYNIC conjugates (**4** and **15**) suggests this is not due solely to the HYNIC chelator. This value does not appear to be an outlier as the duplicate numbers are nearly identical. At this time we have no explanation for the relatively low receptor affinity of **18**.

Divalent DTPA conjugate **17** was radiolabeled with ^{111}In as described in a previous publication to give [^{111}In-(**17**)] (**23**) as shown in Figure 2.[14] The ^{99m}Tc complexes of divalent HYNIC conjugate **18** were prepared from Na-$^{99m}TcO_4$, $SnSO_4$, and one of three coligand systems by heating at 100 °C for 30 min in phosphate-buffered saline, pH 7.0. The three coligand systems (tricine/TPPTS, $tricine_2$, and tricine/ISO) gave complexes **19**, **20**, and **21** as shown in Figure 2. Radiolabeling was rapid and efficient using each of the three coligand systems. The radiochemical purity of all complexes was verified by the analytical methods described in the Experimental Section. While the binary complex (**20**) formed from tricine alone has been used extensively in preclinical research, it suffers from the drawback that it exists in solution in several isomeric forms, many of which are interconverting at room temperature.[28] It would be very difficult to develop such a system for clinical use. In contrast, ternary complexes formed from TPPTS and tricine (e.g., **19**) form only two non-interconverting diastereomeric radiolabeled products when the biomolecule is itself chiral.[12]

Scintigraphic images after injection of divalent ^{99m}Tc complexes **19**, **20**, and **21** are shown in Figure 3. Whole body distribution of the three agents was similar immediately after injection, with significant activity in the lungs and heart (blood pool) and in the kidneys. By 4 h pi, uptake in the abscesses was clearly visible with all three agents, and there was high activity in the kidneys. Images acquired 8 h pi clearly showed that uptake in the abscesses was greater with the tricine/TPPTS and tricine/ISO complexes (**19** and **21**). It was also apparent that kidney uptake was higher with tricine/TPPTS complex **19**. Thus, the images obtained with ternary complex **21** were qualitatively superior to the images obtained with the other divalent ^{99m}Tc complexes. The biodistribution data for complexes **19**, **20**, and **21** at 8 h pi (Figure 4) confirmed these visual impressions. Uptake of **19**, **20**, and **21** in the abscesses was 0.21, 0.08, and 0.22%ID/g, respectively, and the kidney uptake of **19** was nearly twice that of **20** and **21** (0.81, 0.40, and 0.48%ID/g, respectively). In addition, the levels of **19** were slightly higher in the spleen and marrow, and **20** showed slightly slower clearance from the blood. Thus, for this divalent LTB4 antagonist platform, the tricine/ISO coligand system (**21**) combined the highest uptake in the abscess with the lowest uptake in nontarget tissues.

In a final experiment we compared divalent tricine/ISO ternary complex **21** with monovalent tricine/ISO ternary complex **22** and with divalent ^{111}In-DTPA complex **23**. Scintigraphic images 8 h pi are shown in Figure 5. The radioactivity concentration in the abscesses is similar for all three agents, but the kidney concentration appears significantly lower for monovalent complex **22**. This combination of high uptake in the target tissue and low uptake in nontarget tissues makes monovalent [^{99m}Tc(**15**)(tricine)(ISO)] (**22**) the qualitatively superior imaging agent. Initial biodistribution

data for **22** confirms these visual impressions, with abscess uptake 8 h pi of 0.36% ID/g, vs 0.22%ID/g for **21**, as described above. More detailed studies of the pharmacokinetic and imaging properties of **22** will be described elsewhere (manuscript submitted). It is interesting that there is little difference in the images resulting from divalent ^{99m}Tc-HYNIC complex **21** and divalent ^{111}In-DTPA complex. Structurally, the two chelator−radionuclide complexes are very different. It is also interesting that the potential divalent interaction with LTB$_4$ receptors on the cell membrane of the neutrophils did not enhance the accumulation of the either **21** or **23** in the abscess. However, divalent agent [^{99m}Tc(**18**)(tricine)(ISO)] (**21**) did showed enhanced retention in the kidneys as compared to monovalent compound [^{99m}Tc(**15**)(tricine)(ISO)] (**22**). In this instance, divalency did not result in enhanced uptake in the target, but apparently the divalent compound was more efficiently reabsorbed in the renal tubules as has been observed with other HYNIC-conjugated tracers.[29] As a result, abscess-to-background ratios of monovalent compound **22** were higher, resulting in scintigraphic images with improved contrast. See ref 26 for a discussion of the various mechanisms of polyvalent interactions in biological systems.

Conclusions

This study describes the syntheses of three new radiolabeled LTB$_4$ antagonists for imaging infection and inflammation. All three of these tracers visualized intramuscular infection in rabbits within a few hours after injection, and the incorporation of multiple cysteic acid PKMs allowed these tracers to be cleared exclusively via the kidneys. The structural parameters investigated with these tracers included the use of either ^{99m}Tc-HYNIC or ^{111}In-DTPA complexes, monovalent vs divalent LTB$_4$ antagonists, and the coligands used in the ^{99m}Tc-HYNIC complexes. The coligand system had a marked effect on biodistribution in the rabbit model, with the ternary complex using tricine and ISO as coligands (i.e., **21**) providing the best scintigraphic images and the best biodistribution data of the divalent HYNIC derivatives. Monovalent ternary ^{99m}Tc-HYNIC complex **22** gave better scintigraphic images than either divalent ^{99m}Tc-HYNIC complex **21** or divalent ^{111}In-DTPA complex **23**. Tracer **22** appears to be the most promising of these new tracers, combining the highest uptake in abscesses with lowest uptake in nontarget tissues.

Experimental Section

General Methods. Previously published procedures were used for the synthesis of Boc-Csa(Na)-OH,[30] Boc-Glu(OTfp)-Otfp,[31] 6-hydrazinonicotinic acid,[32] LTB$_4$ antagonist **2**,[10] and *N*-(*tert*-butoxycarbonyl)-4,7,10-trioxa-1,13-tridecanediamine.[33] HPLC-grade ACN was obtained from J. T. Baker. Absolute ethanol was obtained from Quantum Chemical Corp. All other reagents and solvents were purchased from Aldrich Chemical Corporation, Lancaster Synthesis, Inc., or Fluka Chemical Corporation and used as received. Merck silica gel, grade 9385, 230−400 mesh, 60 Å was used for flash chromatography. Na-^{99m}TcO$_4$ (Mo-generator) and ^{111}InCl$_3$ were obtained from Tyco Mallinckrodt, Netherlands. All reactions were carried out at ambient temperatures under a nitrogen atmosphere unless noted otherwise. Organic reaction mixtures were concentrated under reduced pressure at 40−65 °C on a rotary evaporator. Reaction monitoring and low resolution mass data were obtained with an Agilent Model 1100 LC/MSD API-electrospray system using either a Phenomenex Synergi Polar-RP C18 column (4 μm, 80 Å, 4.6 × 150 mm) or a Zorbax SB-CN column (5 μm, 4.6 × 150 mm), operated at 50 °C with 0.1% formic acid-modified ACN/water mobile phases. Final HPLC purity determination was made with an Agilent Model 1100 HPLC system, using either a Waters Atlantis dC18 column (5 μm, 4.6 × 100 mm) or a Zorbax SB-CN column (5 μm, 4.6 × 150 mm) and 0.1% TFA or 0.1 M NaOAc-modified ACN/water as mobile phases. UV detection was carried out at 220 and 254 nm. Preparative HPLC purifications were performed on a Varian PrepStar system using SD-1 pumps equipped with a UV/vis detector model 320, using a Waters Atlantis dC18 column (5 μm, 30 × 100 mm) except as noted otherwise and using the gradients and mobile phases given in the text. UV detection was carried out at 220 nm. All chromatography was carried out with HPLC grade organic solvents.

Exact mass determination was performed on a 7.0 T Fourier transform ion cyclotron resonance (FTICR) mass spectrometer (IonSpec Corporation, Lake Forest, CA) equipped with an electrospray ionization source. A mixture of sample and internal calibrant (poly(ethylene glycol) or polypropylene glycol) was prepared at approximately 10 μM each in ACN:water:acetic acid (500:500:1) and infused at 1 μL/min. A spectrum was obtained using the IonSpec OMEGA data system by averaging five transients of 512K data points per transient. Mass calibration was derived from internal calibrant ions bracketing the *m/z* of interest for the sample. FT-NMR spectra were obtained on a Bruker Avance 600 MHz spectrometer at 600 MHz for ^{1}H and 150 MHz for ^{13}C using the indicated solvent. Residual solvent signals were used for internal calibration. Chemical shifts are reported in parts per million (δ), and signals are expressed as s (singlet), d (doublet), t (triplet), q (quartet), p (pentet), m (multiplet), or br (broad). Elemental analyses were performed at Oneida Research Services, Inc, Whitesboro, NY; found values agree favorably with the calculated ones.

Ethyl 5-(5-(5-(4,6-Diphenyl(2-pyridyloxy))-1,1-dimethylpentyl)-1,2,3,4-tetraazolyl)pentanoate (5a). A solution of **2** (35.0 g, 84.6 mmol) and bis(tri-*n*-butyltin) oxide (21.5 mL, 42.3 mmol) in absolute EtOH (1035 mL) was heated at reflux under nitrogen for 30 min. The solution was concentrated under vacuum, and the resulting was dissolved in cyclohexane (3 × 200 mL) and again concentrated to remove traces of EtOH. The oil was dissolved in cyclohexane (35 mL), treated with ethyl 5-bromovalerate (40.0 mL, 254 mmol), and heated at 85 °C in an oil bath under nitrogen for 28 h. The reaction was cooled to ambient temperatures, diluted with ether (350 mL), washed sequentially with 10% KF solution (125 mL) and saturated NaCl (400 mL), dried ($MgSO_4$), and concentrated to give a yellow oil. This oil was purified by silica gel flash chromatography. The column was initially eluted with hexane/EtOAc (75/25) until the unwanted N2 isomer was off the column, and the mobile phase was switched to hexane/EtOAc (60/40) to collect the desired N1 isomer. Product fractions were concentrated and the resulting solid was recrystallized (EtOH) to give 16.58 g (36%) of the title compound as a colorless solid, mp 99.5−101.5 °C. ^{1}H NMR ($CDCl_3$): δ 8.10−8.01 (m, 2H), 7.69−7.62 (m, 2H), 7.55−7.36 (m, 7H), 6.85 (s, 1H), 4.43 (t, J = 6.3 Hz, 2H), 4.34 (t, J = 7.5 Hz, 2H), 4.09 (q, J = 7.1 Hz, 2H), 2.32 (t, J = 7.2 Hz, 2H), 2.07−1.92 (m, 2H), 1.91−1.60 (m, 8H), 1.50 (s, 6H), 1.21 (t, J = 7.1 Hz, 3H); ^{13}C NMR ($CDCl_3$): δ 172.7, 164.1, 159.8, 155.1, 152.1, 139.1, 138.7, 129.0, 128.9, 128.6, 127.0, 126.8, 111.8, 107.1, 65.30, 60.49, 48.57, 41.32, 34.84, 33.40, 29.38, 29.30, 27.17, 21.90, 21.29, 14.18; HRMS: Calcd for $C_{32}H_{40}N_5O_3$ [M + H]$^+$: 542.3131, Found: 542.3140; Anal. ($C_{32}H_{39}N_5O_3$) C,H,N.

Ethyl 5-(4-(5-(4,6-Diphenyl(2-pyridyloxy))-1,1-dimethylpentyl)-1,2,3,5-tetraazolyl)pentanoate (5b). Fractions from the above flash chromatography containing the unwanted N2 isomer were concentrated to give 10.2 g (22%) of the title compound as a colorless solid. ^{1}H NMR ($CDCl_3$): 8.10−8.01 (m, 2H), 7.69−7.61 (m, 2H), 7.55−7.35 (m, 7H), 6.86 (s, 1H),

4.54 (t, J = 7.1 Hz, 2H), 4.42 (t, J = 6.6 Hz, 2H), 4.09 (q, J = 7.1 Hz, 2H), 2.31 (t, J = 7.3 Hz, 2H), 2.09−1.95 (m, 2H), 1.90−1.70 (m, 4H), 1.70−1.56 (m, 2H), 1.45−1.28 (m, 8H), 1.21 (t, J = 7.1 Hz, 3H); ^{13}C NMR ($CDCl_3$): 173.50, 172.81, 164.32, 155.12, 151.97, 139.18, 138.82, 128.94, 128.84, 128.57, 127.03, 126.81, 111.66, 107.10, 65.83, 60.40, 52.32, 42.40, 34.77, 33.32, 29.59, 28.63, 27.21, 21.74, 21.31, 14.18; MS: *m/e* 542.4 [M + H]; HRMS: Calcd for $C_{32}H_{40}N_5O_3$ [M + H]$^+$: 542.3131, Found: 542.3143; Anal. ($C_{32}H_{39}N_5O_3$) C,H,N.

5-(5-(5-(4,6-Diphenyl(2-pyridyloxy))-1,1-dimethylpentyl)-1,2,3,4-tetraazolyl)pentanoic Acid (6). A solution of ester **5a** (16.2 g, 29.9 mmol) in inhibitor free, peroxide free THF (450 mL) was treated with 3 M LiOH (120 mL), and the resulting mixture was stirred rapidly for 19 h. The mixture was concentrated until most of the THF was removed. The resulting aqueous mixture was adjusted to pH 3 with 6 N HCl and extracted with EtOAc (1 × 450, 1 × 60 mL). The combined EtOAc extracts were washed with saturated NaCl (100 mL), dried ($MgSO_4$), and concentrated to give 15.3 g (100%) of the title compound as a viscous colorless oil. ^{1}H NMR ($CDCl_3$): 8.02 (d, J = 8.4 Hz, 2H), 7.65(d, J = 8.2 Hz, 2H), 7.55−7.35 (m, 7H), 6.84 (s, 1H), 4.43−4.31 (m, 4H), 2.36 (t, J = 7.0 Hz, 2H), 2.10−1.92 (m, 2H), 1.89−1.62 (m, 6H), 1.49 (s, 6H), 1.42−1.20 (m, 2H); HRMS: Calcd for $C_{30}H_{36}N_5O_3$ [M + H]$^+$; 514.2818, Found: 514.2819.

***N*-(3-(2-(2-(3-((*tert*-Butoxy)carbonylamino)propoxy)-ethoxy)ethoxy)propyl)-5-(5-(5-(4,6-diphenyl(2-pyridyloxy))-1,1-dimethylpentyl)(1,2,3,4-tetraazolyl))pentanamide (3).** A solution of **6** (5.60 g, 10.9 mmol), DIEA (4.75 mL, 27.3 mmol), and HBTU (5.68 g, 15.0 mmol) in anhydrous DMF (75 mL) was stirred for 5 min and treated with a solution of *N*-(*tert*-butoxycarbonyl)-4,7,10-trioxa-1,13-tridecanediamine (4.81 g, 15.0 mmol) in anhydrous DMF (35 mL). Stirring was continued for 6 h. The DMF was removed, and the resulting viscous oil was partitioned between EtOAc (330 mL) and water (75 mL) at pH 3. The organic phase was washed consecutively with dilute (pH 3) HCl (2 × 75 mL), water (75 mL), saturated $NaHCO_3$ (75 mL), and saturated NaCl (75 mL). The organic phase was dried ($MgSO_4$) and concentrated to give 8.80 g (99%) of **3** as an amber viscous oil. ^{1}H NMR ($CDCl_3$): δ 8.03 (d, J = 8.4 Hz, 2H), 7.65 (d, J = 8.4 Hz, 2H), 7.53 (d, J = 1.2 Hz, 1H), 7.49−7.37 (m, 6H), 6.83 (d, J = 1.2 Hz, 1H), 6.30 (bs, 1H), 4.95 (bs, 1H), 4.41 (t, J = 6.4 Hz, 2H), 4.34 (t, J = 7.5 Hz, 2H), 3.65−3.48 (m, 12H), 3.36−3.25 (m, 2H), 3.21−3.11 (m, 2H), 2.16 (t, J = 7.2 Hz, 2H), 2.02−1.94 (m, 2H), 1.88−1.66 (m, 10H), 1.48 (s, 6H), 1.40 (s, 9H), 1.37−1.28 (m, 2H); ^{13}C NMR ($CDCl_3$): δ 172.06, 170.25, 164.10, 159.91, 157.14, 156.10, 154.98, 152.41, 138.84, 138.58, 129.01, 128.64, 127.59, 127.07, 126.85, 111,90, 78.94, 70.45, 70.42, 70.14, 70.01, 69.93, 69.43, 65.59, 48.72, 41.28, 38.41, 37.88, 35.53, 34.84, 29.70, 29.48, 29.30, 28.90, 28.44, 27.15, 22.59, 21.33; HRMS: Calcd for $C_{45}H_{66}N_7O_7$ [M + H]: 816.5024, Found: 816.5044.

General Procedure for Preactivation of Boc-Csa(Na)-OBt (8). Boc-cysteic acid mono sodium salt in anhydrous DMF (6 mL DMF for 1 mmol Boc-Csa(Na)-OH) was treated with 1 equiv of HBTU and 2 equiv of DIEA, and stirred for 25 min. The resulting solution of active ester was transferred to a solution of the reactive amine using anhydrous DMF to complete the transfer.

LTB$_4$-(Csa)-H (10). A solution of **3** (1.68 g, 2.1 mmol) in 50/40/5/5 DCM/TFA/TIS/H_2O (40 mL) was stirred for 30 min and concentrated yielding **7** as a yellow viscous oil. This oil was dissolved in DMF (25 mL) and made basic with DIEA (2.90 mL, 16.6 mmol). A solution of active ester Boc-Csa(Na)-OBt (**8**) was prepared in a separate flask from Boc-Csa(Na)-OH (1.20 g, 4.1 mmol), HBTU (1.56 g, 4.1 mmol), and DIEA (1.5 mL, 8.6 mmol) in DMF (25 mL). This solution of **8** was added to the solution of **7**, and after 2 h of stirring, the reaction mixture was concentrated, yielding a yellow oil. This oil was redissolved in $CHCl_3$ (180 mL), washed with water (2 × 100 mL), and saturated $NaHCO_3$ (1 × 80 mL). The aqueous layer was back-extracted with $CHCl_3$ (1 × 100 mL). The combined organic layers were dried (Na_2SO_4) and concentrated to give **9** as a pale yellow oily foam. This foam was dissolved in 50/40/5/5 DCM/TFA/TIS/H_2O (40 mL), stirred for 20 min, and concentrated to give mono-cysteic acid derivative **10** as a yellow oil. This oil was used in the subsequent reaction without further purification. MS: *m/z* 867.5 [M + H]$^+$.

LTB$_4$-(Csa)$_2$-H (11). A solution of **10** in DMF (25 mL) and DIEA (2.70 mL, 15.5 mmol) was treated with a solution of Boc-Csa(Na)-OBt (**8**) prepared from Boc-Csa(Na)-OH (1.04 g, 3.6 mmol), HBTU (1.36 g, 3.6 mmol), and DIEA (1.25 mL, 7.2 mmol) in DMF (20 mL). The solution was stirred for 1 h and concentrated to give a viscous yellow oil. This oil was dissolved in 50/40/5/5 DCM/TFA/TIS/H_2O (50 mL), stirred for 20 min, and concentrated. Crude product was purified by HPLC using a 3%/min gradient of 36−72% ACN containing 0.1% TFA at a flow rate of 40 mL/min. The product fraction eluting at 5.7 min was lyophilized to give dicysteic acid derivative **11** (1.03 g, 0.91 mmol, 44% from compound **3**) as a colorless solid. ^{1}H NMR (CD_3OD): δ 7.97−7.94 (m, 2H), 7.94−7.91 (m, 2H), 7.88 (d, J = 1.2 Hz, 1H), 7.63−7.57 (m, 6H), 7.53 (d, J = 1.2 Hz, 1H), 4.87−4.83 (m, 1H), 4.56 (t, J = 6.3 Hz, 2H), 4.50 (t, J = 7.2 Hz, 2H), 4.30 (t, J = 6.0 Hz, 1H), 3.61−3.56 (m, 4H), 3.55−3.50 (m, 4H), 3.48−3.37 (m, 7H), 3.25−3.16 (m, 4H), 3.11−3.05 (m, 1H), 2.24 (t, J = 7.2 Hz, 2H), 1.22−1.88 (m, 6H), 1.75−1.66 (m, 6H), 1.51 (s, 6H), 1.39−1.32 (m, 2H); ^{13}C NMR (CD_3OD): δ 175.4, 171.8, 168.7, 163.4, 161.7, 160.8, 153.4, 137.5, 134.3, 132.7, 132.6, 130.8, 130.6, 129.4, 129.2, 116.1, 106.9, 72.10, 71.63, 71.32, 71.30, 70.06, 69.88, 53.02, 52.74, 51.98, 51.47, 50.21, 42.12, 38.15, 38.11, 36.41, 36.21, 30.63, 30.46, 30.36, 30.06, 27.67, 24.08, 22.3; HRMS: Calcd for $C_{46}H_{68}N_9O_{13}S_2$ [M + H]: 1018.4372; Found: 1018.4386.

LTB$_4$-(Csa)$_3$-H (12). A solution of **11** (911 mg, 0.81 mmol) and DIEA (625 μL, 3.6 mmol) in DMF (10 mL) was treated with solution of Boc-Csa(Na)-OBt (**8**) prepared from Boc-Csa-(Na)-OH (521 mg, 1.8 mmol), HBTU (679 mg, 1.8 mmol), and DIEA (625 μL, 3.6 mmol) in DMF (10 mL). The reaction was stirred for 2 h and concentrated. The residue was dissolved in 50/40/5/5 DCM/TFA/TIS/H_2O (20 mL), stirred for 25 min, and concentrated. Crude product was purified by HPLC using a 3%/min gradient of 31.5−54% ACN containing 0.1% TFA at a flow rate of 40 mL/min. The product fraction eluting at 4.8 min was lyophilized to give tricysteic acid derivative **12** (1.01 g, 0.78 mmol, 97%) as a colorless solid. ^{1}H NMR (CD_3OD): δ 8.03−7.99 (m, 2H), 7.93−7.88 (m, 3H), 7.69−7.59 (m, 7H), 4.72 (dd, J = 3.5, 9.7 Hz, 1H), 4.65 (dd, J = 3.6, 9.6 Hz, 1H), 4.60 (t, J = 6.7 Hz, 2H), 4.54 (t, J = 7.2 Hz, 2H), 4.37 (dd, J = 3.6, 9.6 Hz, 1H), 3.63−3.58 (m, 4H), 3.58−3.53 (m, 4H), 3.53−3.39 (m, 6H), 3.36−3.30 (m, 1H), 3.30−3.19 (m, 7H), 2.36 (t, J = 7.5 Hz, 2H), 2.06−1.99 (m, 2H), 1.99−1.90 (m, 4H), 1.79−1.70 (m, 6H), 1.52 (s, 6H), 1.41−1.33 (m, 2H); ^{13}C NMR (CD_3OD): δ 176.1, 172.4, 171.7, 168.9, 162.9, 162.1, 161.7, 152.6, 136.9, 133.2, 133.0, 132.9, 130.8, 130.7, 129.8, 129.5, 116.7, 106.8, 73.30, 71.53, 71.21, 71.14, 69.91, 69.63, 53.61, 53.04, 52.30, 52.03, 51.73, 50.99, 50.16, 41.93, 38.57, 38.04, 36.18, 36.03, 30.53, 30.19, 30.09, 29.92, 27.63, 24.15, 22.23; HRMS: Calcd for $C_{49}H_{73}N_{10}O_{17}S_3$ [M + H]: 1169.4312; Found: 1169.4309.

LTB$_4$-(Csa)$_4$-H (13). A solution of **12** (705 mg, 0.55 mmol) and DIEA (630 μL, 3.6 mmol in DMF (12 mL)) was treated with a solution of Boc-Csa(Na)-OBt (**8**) prepared from Boc-Csa-(Na)-OH (351 mg, 1.2 mmol), HBTU (457 mg, 1.2 mmol), and DIEA (420 μL, 2.4 mmol) in DMF (7 mL). The reaction was stirred for 40 min and concentrated. The residue was dissolved in 50/40/5/5 DCM/TFA/TIS/H_2O (20 mL), stirred for 25 min, and concentrated. Crude product was purified by HPLC using a 3%/min gradient of 27−54% ACN containing 0.1% TFA at a flow rate of 40 mL/min. The product fraction eluting at 5.3 min was lyophilized to give tetracysteic acid derivative **13** (674.8 mg, 0.47 mmol, 86%) as a colorless solid. ^{1}H NMR (CD_3OD and CD_3CN): δ 7.88−7.83 (m, 4H), 7.77 (d, J = 1.2 Hz, 1H), 7.61−7.53 (m, 4H), 7.34 (d, J = 1.2 Hz, 1H), 4.71 (dd, J = 3.9, 9.3 Hz, 1H), 4.57−4.51 (m, 2H), 4.46−4.39 (m, 4H), 4.37 (dd, J = 4.2, 9.0 Hz, 1H), 3.56−3.34 (m, 14H), 3.31−3.14 (m, 8H), 3.11 (t, J = 6.9 Hz, 2H), 2.17 (t, J = 7.2 Hz, 2H), 1.90 (p, J = 7.5 Hz, 2H), 1.86−1.78 (m, 4H), 1.69 (p, J = 6.6 Hz, 2H), 1.66−1.57 (m, 4H), 1.44 (s, 6H), 1.27−1.20 (m, 2H); ^{13}C NMR (CD_3OD and CD_3CN): δ 175.6, 172.4, 172.0, 171.9, 168.8,

163.3, 161.8, 159.9, 153.2, 137.2, 134.1, 132.7, 132.6, 130.8, 130.6, 129.2, 129.1, 115.8, 106.9, 71.71, 71.11, 70.91, 70.87, 69.80, 69.53, 53.06, 52.88, 52.51, 51.86, 51.67, 51.53, 51.23, 50.95, 50.13, 41.66, 37.87, 37.76, 36.32, 35.98, 30.28, 30.02, 29.84, 29.68, 27.58, 23.83, 21.99; HRMS: Calcd for $C_{52}H_{78}N_{11}O_{21}S_4$ [M + 2H]: 660.7162; Found: 660.7163.

6-(2-Benzaldehydehydrazono)nicotinic Acid (14). A suspension of 6-hydrazinonicotinic acid (274 mg, 1.8 mmol) in DMF (11 mL) was treated with benzaldehyde (1.1 mL, 11 mmol) and stirred for 2 days. Filtration of the reaction mixture gave **14** as a pale yellow powder. The filtrate was diluted with DCM (100 mL) to give an additional crop of **14**. The combined solids were washed with DCM and gave the title compound (284 mg, 1.2 mmol, 66%) as a light yellow powder. ^{1}H NMR (DMSO-d_6 and CD_3OD): δ 8.53 (s, 1H), 8.42 (s, 1H), 8.30 (d, J = 9.0 Hz, 1H), 7.96 (s, 2H), 7.47 (dd, J = 1.8 and 5.4 Hz, 3H), 7.38 (d, J = 9.0 Hz,1H); ^{13}C NMR (DMSO-d_6 and CD_3OD): δ 164.5, 141.9, 133.4, 130.7, 128.8, 127.8, 117.5; HRMS: Calcd for $C_{13}H_{12}N_3O_2$ [M + H]: 242.0924; found: 242.0923.

HYNIC Conjugate 15. A solution of **14** (10.2 mg, 42.3 μmol), PyBOP (19.3 mg, 37.1 μmol), and DIEA (20 μL, 115 μmol) in DMF (0.75 mL) was added to **13** (14.0 mg, 10.6 μmol) in DMF (1.0 mL), and the reaction was stirred for 40 min. Concentration gave crude **15**, which was purified by HPLC using isocratic conditions of 27% ACN containing 0.1 M NaOAc, pH 7 for 2 min at a flow rate of 25 mL/min, followed by a 1.0%/min gradient of 27−54% ACN containing 0.1 M NaOAc, pH 7 at a flow rate of 25 mL/min. The product fraction eluting at 18.1 min was diluted with 3 volumes of H_2O and reloaded on the same preparative HPLC column equilibrated with 4.5% ACN containing 0.1% TFA. The product on the column was desalted by elution with 4.5% ACN containing 0.1% TFA for 15 min at a flow rate of 25 mL/min, followed by a 5.7%/min gradient of 4.5−90% ACN containing 0.1% TFA at a flow rate 25 mL/min. Product fraction eluting a 10.4 min was lyophilized to give HYNIC conjugated monovalent tetracysteic acid derivative **15** (4.9 mg, 3.2 μmol, 30%) as a colorless powder. ^{1}H NMR (CD_3CN and D_2O): δ 8.50 (d, J = 2.1 Hz, 1H), 8.32 (dd, J = 2.1 and 9.0 Hz, 1H), 8.21 (s, 1H), 8.01−7.96 (m, 2H), 7.85−7.80 (m, 2H), 7.78−7.74 (m, 2H), 7.69 (d, J = 1.2 Hz, 1H), 7.53−7.41 (m, 9H), 7.71 (d, J = 9 Hz, 1H), 7.00 (d, J = 1.2 Hz, 1H), 4.88 (dd, J = 4.2 and 9.3 Hz, 1H), 4.65 (dd, J = 4.2 and 8.4 Hz, 1H), 4.58 (dd, J = 4.2 and 8.4 Hz, 1H), 4.52 (dd, J = 4.2 and 8.4 Hz, 1H), 4.37 (t, J = 7.2 Hz, 2H), 4.35 (t, J = 7.8 Hz, 2H), 3.53−3.44 (m, 8H), 3.44−3.35 (m, 5H), 3.35−3.25 (m, 3H), 3.25−3.15 (m, 4H), 3.13 (t, J = 6.6 Hz, 2H), 3.07 (t, J = 6.7 Hz, 2H), 2.11 (t, J = 7.6 Hz, 2H), 1.88−1.78 (m, 4H), 1.74 (p, J = 7.2 Hz, 2H), 1.65 (p, J = 6.6 Hz, 2H), 1.60 (p, J = 6.7 Hz, 2H), 1.57 (p, J = 7.6 Hz, 2H), 1.40 (s, 6H), 1.22−1.14 (m, 2H); ^{13}C NMR (CD_3CN and D_2O): δ 175.9, 172.3, 166.2, 165.1, 163.0, 162.1, 155.7, 152.4, 144.0, 139.1, 138.8, 138.4, 134.5, 132.9, 131.6, 131.5, 130.8, 130.6, 130.5, 129.6, 128.8, 128.7, 122.5, 114.1, 113.7, 107.7, 71.21, 71.17, 71.02, 70.97, 69.98, 69.74, 68.62, 53.14, 53.01, 52.75, 52.17, 52.05, 51.76, 51.70, 50.32, 41.86, 38.07, 37.87, 36.60, 36.20, 30.44, 30.17, 30.12, 29.92, 27.83, 23.99, 22.29; HRMS: Calcd for $C_{65}H_{88}N_{14}O_{22}S_4$ $[M + 2H]^{2+}$: 772.2535; found 772.2535.

(LTB$_4$-(Csa)$_4$)$_2$-Glu-H (16). A solution of **13** (264 mg, 0.18 mmol), Boc-Glu(OTfp)-OTfp (41.2 mg, 0.076 mmol), HOAt (22.7 mg, 0.17 mmol), and DIEA (130 μL, 0.75 mmol) in DMF (2 mL) was stirred for 6 h and concentrated to give a viscous yellow oil. This oil was dissolved in DCM (6.5 mL) and treated with a solution of anisole/H_2O/TFA (0.75 mL/0.75 mL/7 mL) and stirred for 30 min. The reaction solution was concentrated to give crude title compound as a viscous yellow oil. Crude product was purified by HPLC using isocratic conditions of 36% ACN containing 0.1 M NaOAc, pH 7 for 2 min at a flow rate of 25 mL/min, followed by a 0.78%/min gradient of 36−54% ACN containing 0.1 M NaOAc, pH 7 at a flow rate of 25 mL/min. The product fraction eluting at 15 min was diluted with 3 volumes of H_2O, and reloaded on the same preparative HPLC column equilibrated with 4.5% ACN containing 0.1% TFA. The product on the column was desalted by elution with 4.5% ACN containing 0.1% TFA for 15 min at a flow rate of 25 mL/min, followed by a 5.7%/min gradient of 4.5−90% ACN containing 0.1% TFA at a flow rate 25 mL/min. Product fraction eluting a 10 min was lyophilized to give divalent tetracysteic acid derivative **16** (134 mg, 0.047 mmol, 62%) as a colorless solid. ^{1}H NMR (CD_3CN and D_2O): δ 7.78−7.70 (m, 8H), 7.64 (d, J = 1.2 Hz, 2H), 7.59−7.47 (m, 12H), 7.26 (d, J = 1.2 Hz, 2H), 4.72 (dd, J = 3.9 and 9.3 Hz, 1H), 4.65−4.55 (m, 5H), 4.55−4.49(m, 2H), 4.38 (t, J = 7.5 Hz, 4H), 4.33 (t, J = 6.3 Hz, 4H), 3.99 (dd, J = 5.4 and 7.8 Hz, 1H), 3.53−3.43 (m, 16H), 3.42−3.35 (m, 9H), 3.32−3.14 (m, 15H), 3.12 (t, J = 7.2 Hz, 4H), 3.07 (t, J = 7.2 Hz, 4H), 2.51 (t, J = 6.9 Hz, 2H), 2.21−2.11 (m, 5H), 2.09−2.01 (m, 1H), 1.85 (p, J = 7.6 Hz, 4H), 1.81−1.71 (m, 8H), 1.65 (p, J = 6.8 Hz, 4H), 1.60 (p, J = 6.6 Hz, 4H), 1.55 (p, J = 7.4 Hz, 4H), 1.40 (s, 12H), 1.21−1.12 (m, 4H); ^{13}C NMR (CD_3CN and D_2O): δ 175.8, 175.2, 172.3, 172.1, 171.7, 170.2, 162.4, 161.7, 160.2, 152.1, 136.2, 132.9, 132.7, 132.6, 130.6, 130.5, 128.9, 128.8, 115.6, 106.2, 72.02, 70.58, 70.40, 70.35, 69.41, 69.14, 53.94, 52.43, 52.26, 52.17, 52.00, 51.73, 51.56, 51.45, 51.38, 51.23, 50.88, 49.86, 41.12, 37.53, 37.42, 35.99, 35.63, 32.18, 29.75, 29.39, 29.27, 29.10, 27.24, 26.82, 23.42, 21.52; HRMS: Calcd for $C_{109}H_{159}N_{23}O_{44}S_8Na_2$ $[M + 2Na]^{+2}$: 1397.9231; Found: 1397.920.

DTPA Conjugate 17. A solution of **16** (50.1 mg, 0.0182 mmol) and DIEA (64 μL, 0.364 mmol) in anhydrous DMF (2.0 mL) was treated dropwise with a solution of DTPA dianhydride (65.0 mg, 0.182 mmol) and DIEA (16 μL, 0.091 mmol) in anhydrous DMF (3.0 mL) over 10 min. The reaction was quenched after 1.5 h by the addition of water (0.1 mL) and concentrated under vacuum to give a colorless glassy solid. The crude product was purified by HPLC on a Phenomenex Jupiter C18 column (10 μ, 21.2 × 250 mm) using a 0.9%/min gradient of 27−63% ACN containing 0.1% TFA at a flow rate of 20 mL/min. Product fraction eluting at 25.1 min was lyophilized to give **17** as a colorless solid (55.0 mg, 0.0176 mmol, 96%). ^{1}H NMR (D_2O:CD_3CN 1:9): δ 7.58 (d, J = 7.62 Hz, 8H), 7.52−7.36 (m, 14H), 7.04 (s, 2H), 4.74−4.69 (m, 1H), 4.67−4.62 (m, 4H), 4.62−4.56 (m, 4H), 4.54−4.50 (m, 2H), 4.41−4.33 (m, 5H), 4.22−4.08 (m, 12H), 3.64 (s, 2H), 3.53−3.41 (m, 20H), 3.41−3.13 (m, 25H), 3.09 (t, J = 6.75 Hz, 4H), 3.02 (t, J = 6.75 Hz, 4H), 2.42−2.27 (m, 2H), 2.16−2.08 (m, 5H), 1.94−1.86 (m, 1H), 1.84−1.73 (m, 8H), 1.72−1.47 (m, 16H), 1.39 (s, 12H), 1.12−1.04 (m, 4H); HRMS: Calcd for $C_{123}H_{182}N_{26}O_{53}S_8$ $[M + 2H]^{2+}$: 1563.5056; Found: 1563.505.

HYNIC Conjugate 18. A solution of **14** (17.5 mg, 73 μmol), PyBOP (37.8 mg, 72.7 μmol), and DIEA (20 μL, 115 μmol) in DMF (1.0 mL) was stirred for 15 min and added to a solution of **16** (50.0 mg, 17.4 μmol) and DIEA (30 μL, 172 μmol) in DMF (1.0 mL). Stirring was continued for 20 h, and the reaction mixture was concentrated. Crude product was purified by HPLC using isocratic conditions of 40.5% ACN containing 0.1 M NaOAc, pH 7 for 2 min at a flow rate of 25 mL/min, followed by a 0.39%/min gradient of 40.5−49.5% ACN containing 0.1 M NaOAc, pH 7 at a flow rate of 25 mL/min. The product fraction eluting at 11 min was diluted with 3 volumes of H_2O and reloaded on the same preparative HPLC column equilibrated with 4.5% ACN containing 0.1% TFA. The product on the column was desalted by elution with 4.5% ACN containing 0.1% TFA for 15 min at a flow rate of 25 mL/min, followed by a 5.7%/min gradient of 4.5−90% ACN containing 0.1% TFA at a flow rate 25 mL/min. Product fraction eluting a 10.6 min was lyophilized to give HYNIC-conjugated divalent tetracysteic acid derivative **18** (40.2 mg, 13.5 μmol, 78%) as a colorless solid. ^{1}H NMR (D_2O:CD_3CN 1:1): δ 8.58−8.55 (m, 1H), 8.12−8.07 (m, 1H), 8.05−8.00 (m, 4H), 7.98 (s, 1H), 7.73−7.65 (m, 6H), 7.62 (d, J = 1.2 Hz, 2H), 7.50−7.38 (m, 12H), 7.35 (t, J = 7.2 Hz, 2H), 7.32−7.24 (m, 2H), 6.83 (d, J = 1.2 Hz, 2H), 4.75−4.68 (m, 3H), 4.66 (dd, J = 4.6 and 8.3 Hz, 1H), 4.61 (dd, J = 4.6 and 8.1 Hz, 2H), 4.55−4.50 (m, 2H), 4.45 (dd, J = 4.8 and 8.3 Hz, 1H), 4.33 (t, J = 6.9 Hz, 8H), 3.53−3.42 (m, 16H), 3.42−3.10 (m, 28H), 3.07 (t, J = 6.9 Hz, 4H), 2.42 (t, J = 7.6 Hz, 2H), 2.22−2.16 (m, 1H), 2.13−2.07 (m, 4H), 2.07−2.00 (m, 1H), 1.86−1.75 (m, 8H), 1.70 (t, J = 7.2 Hz, 4H), 1.66 (t, J = 6.6 Hz, 4H), 1.60 (t, J = 6.6 Hz, 4H), 1.54 (t, J = 7.6 Hz, 4H), 1.38 (s, 12H), 1.21−1.12 (m, 4H); ^{13}C NMR (D_2O:CD_3CN 1:1): δ

181.22, 175.76, 175.33, 174.19, 172.47, 172.18, 172.00, 171.88, 171.78, 168.97, 165.27, 161.58, 159.24, 156.23, 153.30, 143.78, 139.73, 138.96, 135.84, 130.40, 130.30, 130.19, 129.80, 128.06, 127.78, 121.42, 118.75, 116.81, 112.70, 107.69, 107.46, 70.64, 70.73, 70.47, 70.41, 69.45, 69.25, 66.61, 54.99, 52.40, 52.39, 52.22, 52.05, 52.00, 51.90, 51.68, 51.62, 49.76, 41.39, 37.57, 37.34, 36.08, 35.66, 32.96, 29.93, 29.81, 29.62, 29.41, 27.30, 24.45, 23.45, 21.84; HRMS: Calcd for $C_{122}H_{170}N_{26}O_{45}S_8$ [M + 2H]$^{+2}$: 1487.4784; Found: 1487.482.

Receptor Binding Assay. In vitro binding studies were performed on purified human granulocytes, purified as described previously.[34] Briefly, increasing amounts of **4**, **15**, **17**, or **18**, (0−20 μM) were added to 1×10^8 cells in the presence of 10 000 cpm [^{111}In(**17**)] (0.5 nM) in 0.25 M Tris/HCl, pH 7.2. The cell suspensions were incubated for 1 h at 37 °C, the cells were washed twice (5 min, 5000*g*), supernatant was discarded, and the radioactivity in the pellet (total bound activity) was measured in a shielded well-type gamma counter (Wizard, Pharmacia-LKB, Uppsala, Sweden). The specifically bound fraction versus the LTB_4 antagonist concentration was plotted. The IC_{50} (50% inhibitory concentration) was determined as being the concentration of the LTB_4 antagonist that caused 50% inhibition of the maximum binding of [^{111}In(**17**)].

General Procedure for ^{99m}Tc-Radiolabeling of 18. A solution of **18** (10 μg), $SnSO_4$ (25 μL of a 1 mg/mL solution in 0.1 N HCl), coligand(s), and 110 MBq Na-$^{99m}TcO_4$ in 350 μL of PBS, pH 7.0 was heated for 30 min at 100 °C. Radiochemical purity was checked by instant thin-layer chromatography (ITLC) on silica gel strips (Gelman Sciences, Inc., Ann Arbor, MI) in 0.1 M Na-citrate buffer, pH 6.0. Strips were analyzed in a well-type gamma counter (Wizard, Pharmacia-LKB, Uppsala, Sweden). In addition, RP-HPLC was performed on a C18 column (Zorbax Rx-C18 4.6 mm × 25 cm) on an Agilent 1100 HPLC system equipped with an in-line radio detector (Canberra Packard, Brussels, Belgium), using 5%/min gradient of 0−100% ACN containing 10 mM ammonium acetate pH 7.2 at a flow rate of 1.0 mL/min. The radiolabeling efficiency was >95% in all cases.

[^{99m}Tc(18)(tricine)(TPPTS)] (19). From **18**, tricine (65 μg), and TPPTS (5 mg).

[^{99m}Tc(18)(tricine)$_2$] (20). From **18** and tricine (15 mg).

[^{99m}Tc(18)(tricine)(ISO)] (21). From **16**, tricine (15 mg), and isonicotinic acid (2 mg).

[^{99m}Tc(15)(tricine)(ISO)] (22). A solution of **15** (25 μg), tricine (15 mg), isonicotinic acid (2 mg), $SnSO_4$ (25 μL of a 1 mg/mL solution in 0.1 N HCl), and 555 MBq Na-$^{99m}TcO_4$ in 350 μL of PBS (pH 7.0) was heated for 30 min at 100 °C.

[^{111}In(17)] (23). DPC11870-11 (**17**) (10 μg) was labeled with 37 MBq ^{111}In in metal-free 0.25 M ammonium acetate buffer, pH 5.5 as described previously.[14]

Infection Model. All animal experiments were approved by the local animal welfare committee in accordance with Dutch legislation and carried out in accordance with their guidelines. Nine female New Zealand White (NZW) rabbits weighing 2.3−2.8 kg were kept in cages (one rabbit per cage) and fed standard laboratory chow and water ad libitum. Rabbits were anaesthetized by subcutaneous injection of 0.7 mL of a mixture of 0.315 mg/mL fentanyl and 10 mg/mL fluanison (Hypnorm, Janssen Pharmaceutica, Buckinghamshire, UK). Twenty minutes after administration of anesthesia an *E. coli* infection was induced in the left thigh muscle by intramuscular injection of 4×10^9 colony-forming units of *E. coli* bacteria. Twenty-four hours after induction of the abscess, when swelling of the infected muscle was apparent, three rabbits were intravenously injected with 37 MBq [^{99m}Tc(**18**)-L_1L_2] (3.0 μg), where L_1L_2 equals one of the coligand systems tricine/TPPTS, tricine$_2$, or tricine/isonicotinic acid.

In a following experiment, fifteen animals were divided in three groups of five rabbits. To compare the imaging characteristics of the divalent compounds and the monovalent compound, five animals each were injected with 37 MBq [^{99m}Tc(**18**)(tricine)(ISO)] (**21**), 37 MBq [^{99m}Tc(**15**)(tricine)(ISO)] (**22**), and 11 MBq [^{111}In(**17**)] (**23**) in the lateral ear vein.

Imaging Studies. For scintigraphic imaging, the rabbits were immobilized in a mold and placed prone on a gamma camera (Orbiter, Siemens, Hoffman Estates, IL) using a low-energy parallel hole collimator in case of the ^{99m}Tc-labeled compounds, whereas a medium-energy collimator was used during acquisition of rabbits injected with [^{111}In(**17**)]. Images (300 000 cts/image) were obtained at several time points after injection starting immediately after injection until 8 h postinjection (pi). Images were stored digitally in a 256 × 256 matrix. All images were windowed identically, allowing a fair comparison among the various experiments. At 8 h pi all rabbits were euthanized. A blood sample was taken by cardiac puncture. Tissues were dissected and weighed. The activity in tissues was measured in a shielded well-type gamma counter together with the injection standards and was expressed as the percentage of the injected dose per gram (%ID/*g*).

Statistical Analysis. All mean values are presented as mean ± standard deviation. Statistical analysis was performed using one-way ANOVA. Results were corrected for multiple comparisons with the Bonferroni Multiple Comparisons Test. The level of significance was set at 0.05.

Acknowledgment. The authors thank Mr. Gerry Grutters and Mr. Hennie Eijkholt (University of Nijmegen, Central Animal Laboratory) for technical assistance, and John Pietryka (BMS Medical Imaging) for analytical support.

References

(1) Tager, A. M.; Luster, A. D. BLT1 and BLT2: the leukotriene B_4 receptors. Prostaglandins Leukot. Essent. *Fatty Acids* **2003**, *69*, 123−134.
(2) Yokomizo, T.; Izumi, T.; Chang, K.; Takuwa, Y.; Shimizu, T. A G-protein-coupled receptor for leukotriene B_4 that mediates chemotaxis. *Nature* **1997**, *387*, 620−624.
(3) Yokomizo, T.; Kato, K.; Terawaki, K.; Izumi, T.; Shimizu, T. A second leukotriene B_4 receptor, BLT2. A new therapeutic target in inflammation and immunological disorders. *J. Exp. Med.* **2000**, *192*, 421−432.
(4) Toda, A.; Yokomizo, T.; Shimizu, T. Leukotriene B_4 receptors. *Prostaglandins Other Lipid Mediat.* **2002**, *68−69*, 575−585.
(5) McMillan, R. M.; Foster, S. J. Leukotriene B_4 and inflammatory disease. *Agents Actions* **1988**, *24*, 114−119.
(6) Brooks, C. D.; Summers, J. B. Modulators of Leukotriene Biosynthesis and Receptor Activation. *J. Med. Chem.* **1996**, *39*, 2629−2654.
(7) van Eerd, J. E.; Boerman, O. C.; Corstens, F. H.; Oyen, W. J. Radiolabeled chemotactic cytokines: new agents for scintigraphic imaging of infection and inflammation. *Q. J. Nucl. Med.* **2003**, *47*, 246−255.
(8) Bleeker-Rovers, C. P.; Boerman, O. C.; Rennen, H. J.; Corstens, F. H.; Oyen, W. J. Radiolabeled compounds in diagnosis of infectious and inflammatory disease. *Curr. Pharm. Des.* **2004**, *10*, 2935−2950
(9) Harris, T. D.; Glowacka, D.; Kalogeropoulos, S. A.; Edwards, D. S.; Liu, S.; Barrett, J. A.; Heminway, S. Synthesis and evaluation of Tc-99m labeled LTB_4 antagonist as potential infection/inflammation imaging agents. *Abstracts of Papers,* 216th National Meeting of the American Chemical Society, Boston, MA, Aug 23-27, 1998; American Chemical Society: Washington, DC, 1998; U211−U211 035.
(10) Labaudiniere, R.; Dereu, N.; Cavy, F.; Guillet, M.; Marquis, O.; Terlain, B. ω-[(4,6-Diphenyl-2-pyridyl)oxy]alkanoic Acid Derivatives: A New Family of Potent and Orally Active LTB_4 Antagonists. *J. Med. Chem.* **1992**, *35*, 4315−4324.
(11) Harris, T. D.; Sworin, M.; Williams, N.; Rajopadhye, M.; Damphousse, P. R.; Glowacka, D.; Poirier, M. J.; Yu, D. Synthesis of Stable Hydrazones of a Hydrazinonicotinyl-Modified Peptide for the Preparation of ^{99m}Tc-Labeled Radiopharmaceuticals. *Bioconjugate Chem.* **1999**, *10*, 808−814.
(12) Edwards, D. S.; Liu, S.; Barrett, J. A.; Harris, A. R.; Looby, R. J.; Ziegler, M. C.; Heminway, S. J.; Carroll, T. R. New and Versatile Ternary Ligand System for Technetium Radiopharmaceuticals: Water Soluble Phosphines and Tricine as Coligands in Labeling a Hydrazinonicotinamide-Modified Cyclic Glycoprotein IIb/IIIa Receptor Antagonist with ^{99m}Tc. *Bioconjugate Chem.* **1997**, *8*, 146−154.
(13) Brouwers, A. H.; Laverman, P.; Boerman, O. C.; Oyen, W. J.; Barrett, J. A.; Harris, T. D.; Edwards, D. S.; Corstens, F. H. A ^{99m}Tc-labeled leukotriene B_4 receptor antagonist for scintigraphic detection of infection in rabbits. *Nucl. Med. Commun.* **2000**, *21*, 1043−1050.

(14) van Eerd, J. E.; Oyen, W. J.; Harris, T. D.; Rennen, H. J.; Edwards, D. S.; Liu, S.; Ellars, C. E.; Corstens, F. H.; Boerman, O. C. A bivalent leukotriene B(4) antagonist for scintigraphic imaging of infectious foci. *J. Nucl. Med*. **2003**, *44*, 1087−1091

(15) Isida, T.; Akiyama, T.; Nabika, K.; Sisido, K.; Kozima, S. The Formation of Tin−Nitrogen Bonds. V. The Selective 1-Substitution Reaction of Tetrazoles by the Reaction of 5-substituted 2-(Tri-*n*-butylstannyl)tetrazoles with Methyl Iodide, Methyl *p*-Toluenesulfonate, Dimethyl Sulfate, and Ethyl Bromoacetate. *Bull. Chem. Soc. Jpn.*, **1973**, *46*, 2176−2180.

(16) Edwards, D. S.; Liu, S.; Ziegler, M. C.; Harris, A. R.; Crocker, A. C.; Heminway, S. J.; Barrett, J. A.; Bridger, G. J.; Abrams, M. J.; Higgins, J. D. 3rd. RP463: a stabilized technetium-99m complex of a hydrazino nicotinamide derivatized chemotactic peptide for infection imaging. *Bioconjugate Chem*. **1999**, 884−91.

(17) Djuric, S. W.; Fretland, D. J.; Penning, T. D. The Leukotriene B_4 receptor antagonists: A most discriminating class of antiinflammatory agent? *Drugs Future*. **1992**, *17*, 819−830.

(18) Cohen, N.; Yagaloff, K. A. Recent progress in the development of Leukotriene B_4 antagonists. *Curr. Drugs* **1994**, 13−22.

(19) Lin, K. S.; Luu, A.; Baidoo, K. E.; Hashemzadeh-Gargari, H.; Chen, M. K.; Brenneman, K.; Pili, R.; Pomper, M.; Carducci, M. A.; Wagner, H. N., Jr. A New High Affinity Technetium-99m-Bombesin Analogue with Low Abdominal Accumulation. *Bioconjugate Chem*. **2005**, *16*, 43−50.

(20) Chen, X.; Park, R.; Shahinian, A. H.; Bading, J. R.; Conti, P. S. Pharmacokinetics and tumor retention of ^{125}I-labeled RGD peptide are improved by PEGylation. *Nucl. Med. Biol*. **2004**, *3*, 11−9.

(21) Decristoforo, C.; Mather, S. J. The influence of chelator on the pharmacokinetics of ^{99m}Tc-labeled peptides. *Q. J. Nucl. Med*. **2002**, *46*, 195−205. Review.

(22) Rennen, H. J.; van Eerd, J. E.; Oyen, W. J.; Corstens, F. H.; Edwards, D. S.; Boerman, O. C. Effects of coligand variation on the in vivo characteristics of Tc-99m-labeled interleukin-8 in detection of infection. *Bioconjugate Chem*. **2002**, *13*, 370−377.

(23) Su, Z.; He, J.; Rusckowski, M.; Hnatowich, D. J. In Vitro Cell Studies of Technetium-99m Labeled RGD-HYNIC Peptide, A Comparison of Tricine and EDDA as Co−Ligands. *Nuc. Med. Biol*. **2003**, *30*, 141−149.

(24) Barrett, J. A.; Cheesman, E. H.; Harris, T. D.; Rajopadhye, M. Radiopharmaceuticals for Imaging Infection and Inflammation. U.S. Patent 6,416,733, 2002.

(25) Butler, R. N. Recent advances in tetrazole chemistry. *Adv. Heterocycl. Chem.* **1977**, *21*, 323−435.

(26) Mammen, M.; Choi, S.; Whitesides, G. M. Polyvalent Interactions in Biological Systems: Implications for Design and Use of Multivalent Ligands and Inhibitors. *Angew. Chem., Int. Ed.* **1998**, *37*, 2754−2794.

(27) Janssen, M.; Oyen, W. J.; Massuger, L. F.; Frielink, C.; Dijkgraaf, I.; Edwards, D. S.; Radjopadhye, M.; Corstens, F. H.; Boerman, O. C. Comparison of a monomeric and dimeric radiolabeled RGD-peptide for tumor targeting. *Cancer Biother. Radiopharm*. **2002**, *17*, 641−646.

(28) Liu, S.; Edwards, D. S.; Looby, R. J.; Harris, A. R.; Poirier, M. J.; Barrett, J. A.; Heminway, S. J.; Carroll. T. R. Labeling a Hydrazino Nicotinamide-Modified Cyclic Iib/IIIa Receptor Antagonist with ^{99m}Tc Using Aminocarboxylates as Coligands. *Bioconjugate Chem*. **1996**, *7*, 63−71.

(29) Decristoforo, C.; Melendez-Alafort, L.; Sosabowski, J. K.; Mather, S. J. ^{99m}Tc-HYNIC-[Tyr3]-octreotide for imaging somatostatin-receptor-positive tumors: preclinical evaluation and comparison with 111I*n*-octreotide. *J. Nucl. Med*. **2000**, *41*, 1114−9.

(30) Hubbuch, A.; Danho, W.; Zahn, H. Synthesis of N−Protected Cysteic Acid Derivatives and Their Activated Esters. *Liebigs Ann. Chem.* **1979**, 776−783.

(31) Harris, T. D.; Barrett, J. A.; Carpenter, A. P.; Rajopadhye, M. Vitronectin receptor antagonist pharmaceuticals. U.S. Patent 6,-511,649, B1, 2003.

(32) Schwartz, D. A.; Abrams, M. J.; Giademenico, C. M.; Zubieta, J. A. Certain Pyridyl Hydrazines and Hydrazides Useful for Protein Labeling. U.S. Patent 5,206,370, 1993.

(33) Wilbur, D. S.; Hamlin, D. K.; Buhler, K. R.; Pathare, P. M.; Vessella, R. L.; Stayton, P. S.; To, R. Streptavidin in Antibody Pretargeting. 2. Evaluation of Methods for Decreasing Localization of Streptavidin to Kidney while Retaining Its Tumor Binding Capacity. *Bioconjugate Chem*. **1998**, *9*, 322−330.

(34) van der Laken, C. J.; Boerman, O. C.; Oyen, W. J.; van de Ven, M. T.; Edwards, D. S.; Barrett, J. A.; van der Meer, J. W.; Corstens, F. H. Technetium-99m-labeled chemotactic peptides in acute infection and sterile inflammation. *J Nucl. Med.* **1997**, *38*, 1310−1315.

JM050383H